Front. Earth Sci. 2014, 8(1): 142–149
DOI 10.1007/s11707-013-0370-2

RESEARCH ARTICLE

A typical flat-panel membrane bioreactor with a composite membrane for sulfur removal

Jian GUAN (✉)[1], Yuan XIAO[1], Jimin SONG[2], Junhe MIAO[2]

1 China Special Equipment Inspection and Research Institute, Beijing 100013, China
2 Shenyang Institute of Special Equipment Inspection and Research, Shenyang 110035, China

Abstract The aim of this work was to provide a concrete study to understand the effects of operation on biofilm morphology and microstructure and degradation efficiency for the disposal of sulfur dioxide produced by coal-fired power plants. For this purpose, a flat-panel reactor–membrane bioreactor (MBR) with a composite membrane consisting of a dense layer and a support layer was designed; the membrane bioreactors inoculated with *Thiobacillus ferrooxidans* were further conducted for the removal of sulfur dioxide. Dry weight, active biomass, pressure drop, removal efficiency, morphology and structure of the formed biofilms were investigated and analyzed over period of biofilm formation. The results found that the dry weight, biomass, pressure drops and removal efficiency increased rapidly during biofilm formation, remained relatively stable in the stabilization period of biofilm growth, and finally reached 0.085 g, 7.00 μg, 180 Pa, and 78%, respectively. Our results suggested the MBR is available for flue-gas desulfurization.

Keywords membrane bioreactor, biofilm, flue gas desulfurization, biodegradation, sulfur dioxide

1 Introduction

As the biggest energy consumers in the world at present, types of energy used in China has always been of great concern to the world (Yang and Chen, 2011, 2012). Coal has always dominated China's electronic generation, even in the near future. The production and utilization of coal in China have previously been shown to have a lot of negative effect on environment (Chen and Chen, 2006a, b). The process of the coal production is described as "a fire, a stream of fumes and a pile of ashes" (Chen et al., 2007). Emission of sulfur dioxide (SO_2) has been considered as important environment pollution accompanied by coal-fired power plants (Bhadra et al., 1987; Chen and Chen, 2009). SO_2 is not only one pollutant to the natural environment, but also a serious threat to the human health (Chen et al., 2006a, b; Chen and Chen, 2007; Chen and Chen, 2012b; Chen et al., 2012d). By the end of 2003, the total installation capacity of electronic power in China had reached to 2.9 billion kW and annual amount of SO_2 emission reached to about 1 million tons (Sun and Zhong, 2005; Chen et al., 2010; Dai et al., 2012), a value that is increasing and expected to further develop (Chen and Chen, 2012a). The direct discharge of pollutants (i.e., SO_2) will cause serious environmental pollution (Chen et al., 2009, 2011; Richard et al., 2011; Chen et al., 2012c). Therefore, effective method to remove or absorb SO_2 has always been the key question for environmental protection.

Numerous traditional techniques including magnesia flue gas desulfurization (FGD), dual alkalis, sodium citrate, phosphate ammoniate fertilizer, electron irradiation, charged dry sorbent injection, limestone injection into the furnace, limestone injection into circulating fluid bed (CFB) and bio-desulfurization have been used to treat sulfur in waste gas streams (Ali et al., 1992; Więckowska 1995; Kusnierova et al., 2010; Pysh'yev et al., 2012). These techniques generally have their disadvantages, such as high cost, secondary pollution and complex control procedures (Liu et al., 2008; Liu et al., 2009; Qu et al., 2009a, b).

In contrast, biological treatment could totally change the components of waste material rather than physically state change, and they have the potential of low-cost implementation (Eligwe, 1988; Chen et al., 2004; Zhao et al., 2009a,b; Yu et al., 2012). A membrane bioreactor (MBR) system for the treatment of waste air can isolate liquid from gas during the process of treatment (Chen et al., 2012a, b). Pollutants diffuse through the membrane and are subse-

Received January 8, 2013; accepted March 6, 2013

E-mail: guanpipe@sina.com

quently degraded by microorganisms in the biofilm (Bos et al., 1988). Because of the separation of liquid and air, waste air containing hydrophobic compounds can be treated effectively (Zhan et al., 2012). Nutrients are present in the liquid phase, and the differences in the concentration between the gas phase and liquid phase provides the driving force for diffusive transport across the membrane (Zhang et al., 2008; Zhang et al., 2012). Since the liquid phase is continuously recirculated, the pH can easily be corrected and toxic degradation products can be removed (Su et al., 2012). In a composite membrane bioreactor, the biofilm forms on the dense side of the membrane.

An advantage of the membrane bioreactor over the biofilter is the presence of a discrete water phase allowing optimal humidification of the biomass and removal of degradation products (Evrim et al., 1998; Chen et al., 2008), these could avoid the inactivation of the biomass (Iranpour et al., 2005; Wang et al., 2009a; Zhao et al., 2009b; Yang et al., 2010; Xu et al., 2011). Moreover, membrane reactors do not contain moving parts and are easy to scale up (Zhou et al., 2009; Yang et al., 2010; Zhang et al., 2011), and the flows of gas and liquid can be varied independently, without problems of flooding, loading, or foaming, which were always detected in bubble columns (Pereira et al., 2002; Jiang et al., 2007, 2008, 2009).

Although the treatment of waste gas through MBR has rapidly developed in the field of environmental protection, further work regarding the characteristics of the bioreactor are urgently needed (Zhang et al., 2009; Zhao et al., 2009a, b; Lu et al., 2012). Experimental investigations show that the operations have a great impact on biofilm formation in the MBR with respects to the treatment of waste gas from coal-fired power plants, which affects the stable operation and removal efficiency (Howell, 2004; Ji et al., 2009; Lu et al., 2012; Su et al., 2012).

In this work, a flat-panel MBR with a composite membrane consisting of two layers (i.e., a dense layer and a support layer) was designed and fabricated for sulfur removal. During biofilm formation, the dry weight, active biomass, pressure drop and removal efficiency were investigated, and then morphology and structure of the formed biofilms were further analyzed to elucidate the effects of operation on biofilm formation and degradation performance.

2 Materials and methods

2.1 Materials and microorganism cultivation

A carbon-cloth composite membrane (effective membrane area 40 cm^2) with hydrophobic treatment was used. Polytetrafluoroethyl (PTFE) was used as the hydrophobic dense top layer and carbon cloth as the support layer (Zhang et al., 2009; Yang et al., 2011b, 2012). The membrane was incorporated into a Perspex reactor module (Huang et al., 2012). Indigenous *Thiobacillus ferrooxidans* bacteria circulated in the bioreactor for sulfur degradation was isolated from local sulfur ore (Olsson et al., 1989; Feng et al., 2011). The bacteria was grown in a synthetic medium consisting of 33.4 g/L $FeSO_4$, 6 g/L $(NH_4)_2SO_4$, 0.2 g/L KCl, 1.0 g/L $MgSO_4$, and 0.02 g/L $Ca(NO_3)_2$ (Bai et al., 2011; Song et al., 2012). For the pre-culture, the sulfur source was sulfur powder. The cells were aerobically cultivated at 30°C on a HY vertical multi-purpose vibrator (Zeng et al., 2012). The initial pH of the medium prior to the incubation was adjusted to 3.0 (Wang et al., 2005; Liu et al., 2009; Hubacek et al., 2012). Enriched bacteria were initially used as the inoculum for start up of the bioreactor. For all the experiments described herein, the MBR was rinsed with deionized water and the mineral medium and heat-resistant reactors were decontaminated with ultraviolet sterilization prior to the experiments (Huang et al., 2007; Ju and Chen, 2011; He et al., 2013). This ensured that the microorganism cultivated was still the dominant organism in the system.

2.2 Laboratory-scale membrane biofilm reactor set-up and operating conditions

The scheme of the experimental system is shown in Fig. 1. The MBR consisted of two parts in a Perspex reactor module. Each part had only one channel (liquid side: 20 cm height×20 mm length×5 mm depth, gas side: 20 cm height×20 mm length×2 mm depth). The membrane was clamped between the two identical Perspex reactor halves. Sulfur dioxide was continuously dosed to the inlet air stream using a gas cylinder. Sulfur dioxide was then transported to a mixing chamber at the same time, another inlet air stream controlled by a mass flow controller was also transported to the chamber. This system was designed to regulate the concentration. A mass flow controller connected to a regulator was used to provide metered flow of synthetic waste air to the reactor. The resulting synthetic waste gas was introduced to the reactor. Throughout the experiments, the sulfur dioxide inlet concentration was generally maintained at 1 g/m^3. The effective membrane area was 40 cm^2, and the volume of each compartment was 20 mL (liquid side) and 8 mL (gas side). The membrane biofilm reactor was placed in an isothermal chamber and kept at (30±0.1) °C. An aqueous mineral medium with inoculum liquid phase (in 33.4 g/L $FeSO_4$, 6 g/L $(NH_4)_2SO_4$, 0.2 g/L KCl, 1.0 g/L $MgSO_4$, and 0.02 g/L $Ca(NO_3)_2$) was continuously recirculated along the dense side at a flow rate of 20 mL/min by a peristaltic pump. Between the pump and module, a pulse dampener was placed. The mineral medium was magnetically stirred at 500 rpm. All chemicals for the mineral medium were of high-purity grade (>99.9% pure). Through the other compartment, contaminated air passed along the porous membrane side in countercurrent with the liquid stream. A

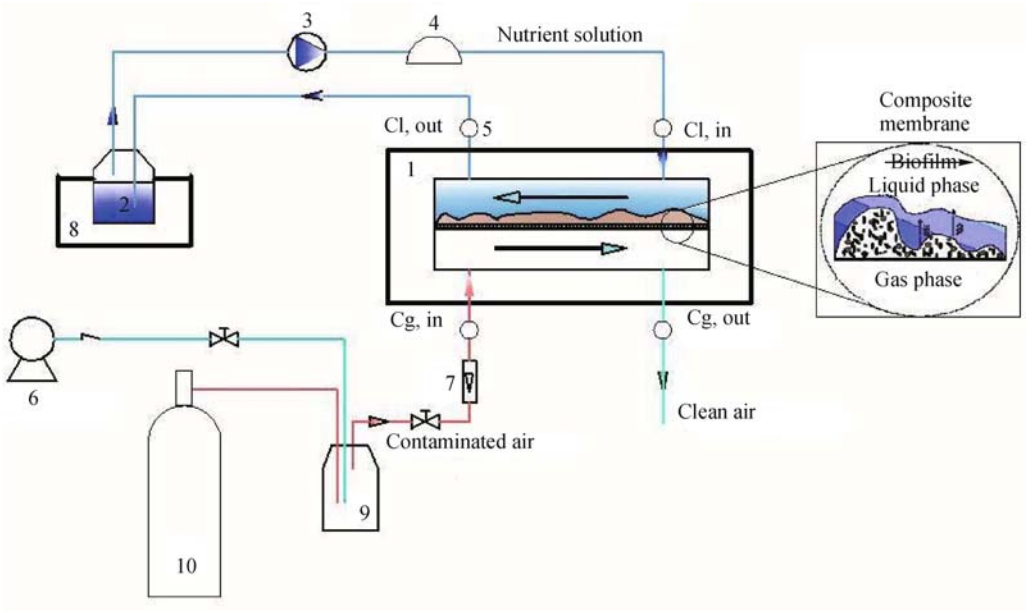

Fig. 1 Schematic diagram of the experimental setup. 1. Menbrane bioreactor; 2. Module; 3. Pulse dampener; 4. Peristaltic pump; 5. Globe valves; 6. Gas cylinder; 7. Flow meter; 8. Isothermal chamber; 9. Gas collecting bottle; 10. Cylinder.

gas flow rate of 40 mL/min was selected, corresponding to gas residence time of 12 s.

The membrane bioreactor was inoculated by circulating a batch culture along the dense side of the membrane. The reactor was inoculated with indigenous *T. ferrooxidans* bacteria. Substrate was only added on the gas side of the membrane, resulting in the microorganisms attaching to the PTFE layer. The biofilm structure was the main research object. Meanwhile, the sulfur degradation rate, dry weight, active biomass, and pressure drop with biofilm formation were measured to analyze the start up of biofilm formation.

2.3 Bioreactor performance

The reactor was seeded with indigenous *T. ferrooxidans* bacteria, which had been grown in a mineral medium with sulfur as the sole energy source. The loading rate, elimination capacity and removal efficiency of sulfur dioxide during the operation period are shown in Fig. 1. Air flow rates and sulfur dioxide feeding controlled by the mass flow regulator determined the gas residence time and sulfur dioxide loading rate in the membrane bioreactor. The performance of the membrane bioreactor was evaluated according to removal efficiency and elimination capacity. These parameters are defined as

Removal Efficiency:

$$RE = \frac{C_{in} - C_{out}}{C_{out}} \times 100. \quad (1)$$

Elimination Capacity:

$$EC = Q \times \frac{C_{in} - C_{out}}{V}. \quad (2)$$

2.4 Analysis methods

The toluene content in the MBR system was determined with a gas chromatograph (SC-2000, Chongqing, China) equipped with a thermal conductivity detector (TCD) and a 3-m stainless-steel column packed with porous styrene particles. Nitrogen and hydrogen with flow rate of 30 mL/min were used as the carrier gas, and the temperatures of the gas chromatograph oven and TCD were maintained at 80°C and 200°C, respectively. The electric current for the TCD was 80 mA. The medium was weighed with an analytical balance (Sartorius BP114, Germany), and the pH measured with an Ecoscan-pH6 m (Singapore). The liquid pressure loss was measured with a Validyne Dp15-22 pressure sensor.

The morphology and microstructure of biofilms that formed under different toluene concentration conditions were analyzed by scanning electron microscopy (SEM) (using a HITACHIS-3400N instrument). The samples were pretreated as follows. A sample of biofilm was extracted from part of the membrane covered with biofilm and fixed on the solid matrix using phosphate buffered saline with 2.5% glutaraldehyde (pH 7.2–7.4). Metal impregnation was carried out by transferring the glutaraldehyde-fixed sample to OsO_4 in the phosphate buffer, and the sample was then washed with the same buffer. The fixed samples were dehydrated stepwise with a graded series of ethanol solutions (30%, 50%, 70%, 80%, 90%, and 100%), then

critical-point dried with tert-butyl ethanol and sputter coated with a thin layer of gold. The biofilm was observed in high vacuum by SEM in secondary electron imaging mode.

The microbial biomass was determined by a phospholipid analysis procedure. The procedure comprised the following steps. (i) Half of the membrane was added to 50-mL screw-cap test tubes. Then, 5 mL of chloroform, 10 mL of methanol and 4 mL of deionized water were added to the samples. The extraction mixture was gently shaken for 10 min and allowed to stand to complete the phase separation. (ii) Samples were added 5 mL of chloroform and 5 mL of deionized water. The aqueous (upper) phase was aspirated from the test tubes with the aid of a glass syringe and subsamples of 3 mL of the chloroform layer were transferred into 10-mL screw-cap test tubes. (iii) The chloroform was removed under a stream of nitrogen, and phosphate was liberated from lipids by adding 3 mL of a potassium persulfate solution and the sealed test tubes were heated in an oven at 105°C for 2 hr. (iv) A 0.45-mL sample was transferred in a cuvette and phosphate release through persulfate digestion was determined by adding 0.1 mL of an ammonium molybdate solution (2.5% of $(NH_4)_6Mo_7O_{24}\cdot 4H_2O$ in 5.72 N H_2SO_4 allowed to stand for 10 min) and 0.45 mL of a malachite green solution (0.111% polyvinyl alcohol (MW 22,000) dissolved in water at 80°C is allowed to cool, and 0.011% malachite green oxalate salt is then added and allowed to stand for 30 min). (v) The absorbance at 610 nm was then recorded using a spectrophotometer (756MC, Shanghai, China). The concentrations of phosphate were calculated based on a regression analysis. The biomass concentration was calculated with a conversion factor of 191.7 μg of biomass-C per 100 mmol of phospholipid and a conversion factor of 2 g biomass-volatile suspended solids (VSS) per gram of biomass-C according to an empirical formula for sludge organisms.

The dry weight of biofilm was measured using the following procedure. Mature biofilm adhering to the membrane was washed gently with distilled water to eliminate non-fixed biomass and then dried at 105°C to a constant weight. The dry weight of biofilm was evaluated as the difference between the weight of the cover glass slide with dry cells and the weight of the bare cover glass slide. An optical microscope with micrometer was employed to measure the biofilm thickness as the average of thickness measurements at 10 points uniformly distributed over the cover glass slide with attached biofilm.

3 Results and discussion

The sulfur dioxide diffusing through the membrane and subsequently degraded by the microorganisms is the sole sulfur source for the microorganisms and the concentration of toluene greatly affects biofilm formation. To study the process of biofilm formation, cells were immobilized on the membrane under a sulfur dioxide concentration of 1 g/m^3, at a constant gas flow rate (40 mL/min) and liquid flow rate (20 mL/min).

3.1 Pressure drops

Biofilm formation in an MBR is within a finite volume. Biofilm reduces the effective cross-sectional area on the liquid side and increases surface roughness, which can transform the flow resistance in the liquid circulation cavity. Therefore, pressure drops of the liquid phase were measured to reflect the growth status of the biofilm in the start-up process.

The variations in pressure drops in the liquid phase are shown in Fig. 2. The pressure drops increased initially, and thereafter remained relatively constant at 180 Pa. Further observations found that the pressure drops were initially low and then rose rapidly. This was due to the increased concentration of microorganism and absorption of microorganisms on the membrane that resulted in a rise of the pressure drop. Five days later, the rapid growth of biofilm, the rise of the flow surface roughness and the gradually increasing thickness of the biofilm reduced the liquid cross-sectional area and increased the flow resistance. All these factors led to a continuous increase in the pressure drop in the liquid phase. Until the 11th day, the pressure drops tended to be steady overall. Meanwhile, the thickness of biofilm and D600-nm value of the circulation liquid reached a steady-state. Finally, the pressure drop remained relatively stable.

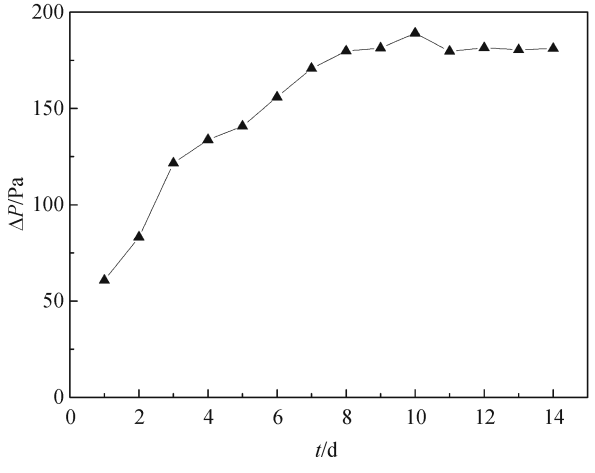

Fig. 2 Pressure drop between the liquid inlet and outlet of MBR bioreactor during biofilm formation period.

3.2 Removal efficiency and elimination capacity of SO_2

Removal efficiency is the ratio between elimination capacity and the loading rate of contaminant, and it can directly illustrate the degradation performance of the

biofilm and the capacity of the MBR in flue gas desulfurization. Therefore, the removal efficiency and elimination capacity are two important parameters which could demonstrate the start-up process. The variations in sulfur degradation performance of biofilm is shown in Figs. 3 and 4. The removal efficiency and elimination capacity both increased over time, where they were 60% and 150 $g \cdot m^{-3} \cdot hr^{-1}$ respectively at the beginning of growth season.

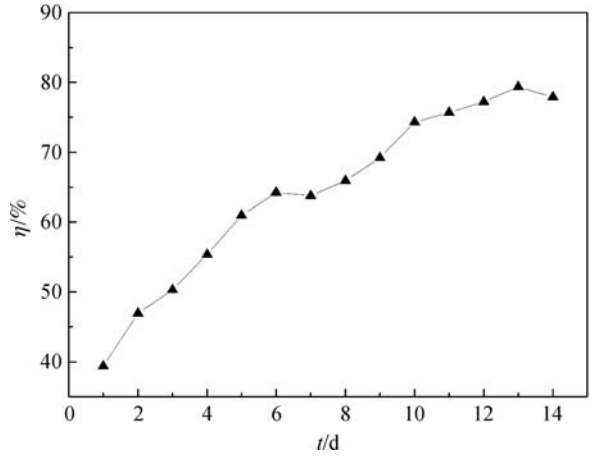

Fig. 3 Removal efficiency of MBR over period of biofilm formation.

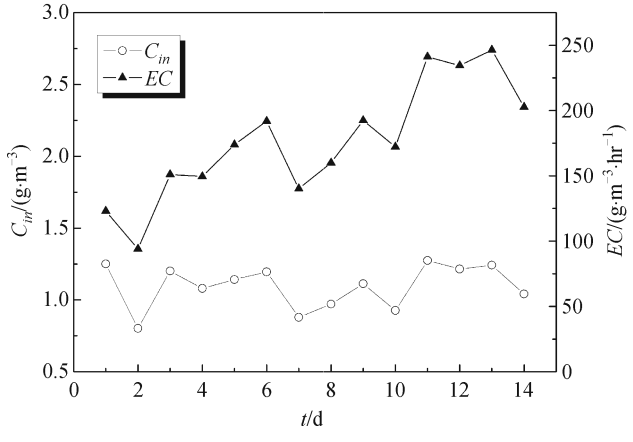

Fig. 4 Inlet concentration and elimination capacity of MBR over period of biofilm formation.

In the start-up process, both the removal efficiency and elimination capacity rapidly increased. After 11 days, the removal efficiency remained at 78% and the elimination capacity at a level of 230 $g \cdot m^{-3} \cdot hr^{-1}$. This is attributed mainly to the growth of the biofilm at the beginning of biofilm formation, and the amount of biomass restricted the biodegradation capacity. As biofilm formation continued, more and more microorganisms were absorbed onto the membrane and formed biofilm. Sulfur dioxide diffused through the membrane and was subsequently degraded by the microorganisms. The effective biodegradation of sulfur dioxide enhances the concentration gradient between the gas phase and liquid phase, which further increases the mass transfer rate and the degradation of the sulfur dioxide by the biofilm. Hence, both the removal efficiency and elimination capacity increased. In comparison, the biofilm became mature and the MBR maintained at a high level of degradation later in the period of biofilm formation.

The overall process of biofilm formation reflects that the concentration of inlet sulfur dioxide and removal efficiency exert a great affect on the elimination capacity. The elimination capacity is an important parameter for assessing the performance of a MBR system. At the beginning of biofilm formation, the rapid increase in removal efficiency enhanced the elimination capacity. The elimination capacity reaches a steady-state as the biofilm matures, which is very similar to the case of removal efficiency.

3.3 Dry weight

Dry weight is another important parameter that reflects the growth of microorganisms on the membrane. Dry weights of MBR over period of biofilm formation are shown in Fig. 5. Dry weight increased over period of biofilm formation. However, the growth rates are different during the growth season. There is rapid growth from the second day to the sixth day, where dry weight increased from 0.0012 to 0.049 g. This is mainly attributed to the sufficient nutrition in the recirculated mineral medium, which guaranteed the nutrient supply for the rapid growth of microorganisms. Meanwhile, the requirement of sulfur dioxide also increased and the removal efficiency rapidly rose from the second day to the sixth day. , the growth rate of dry weight slowed down after six days. On the 13th day,

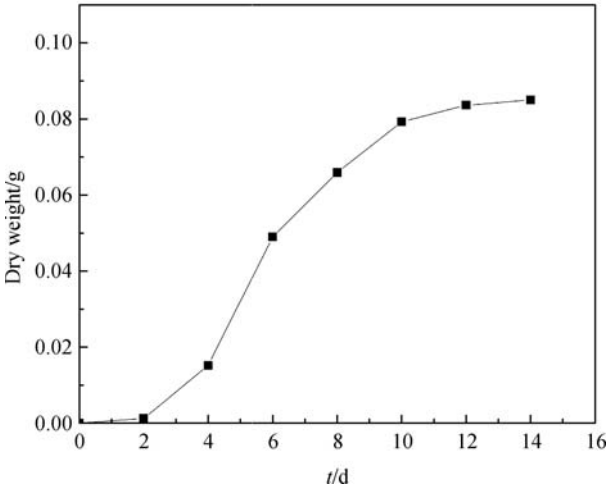

Fig. 5 Development of dry weight of MBR over period of biofilm formation.

the dry weight remained relatively stable with the final value of 0.085 g, mature biofilm formed.

3.4 Biomass

Biomass is a key parameter for the evaluation of the growth of biofilm. It directly affects the biodegradation performance of a MBR.

As the activity of microorganisms decreases, phospholipids in microorganisms rapidly decompose. Therefore, hydrolysis polyphosphate is used to evaluate the active biomass and characterize the microorganisms in biofilm.

The change of biomass over period of biofilm formation is shown in Fig. 6. The biomass initially increased fast, and thereafter leveled off. There was little active biomass during the first two days, and the amount slowly increased from 0 to 0.098 μg. From the second day to the sixth day, biomass increased very fast from 0.098 μg to 4.03 μg, probably due to sufficient nutrition and sulfur dioxide the microorganisms absorbed on the membrane. The growth rate of biomass decreased later over period of biofilm formation. This is because the increase in mass transfer resistance and the reduction of the average concentration of sulfur dioxide, which slowed the growth of the microorganisms. Additionally, the concentration of nutrients and the driving force decreased over period of biofilm formation because of the consumption of the substrate. The sulfur dioxide passed through the membrane by the concentration gradient and was degraded by the microorganisms. When the growth and death of the microorganisms in biofilm reached equilibrium, a mature biofilm formed finally. A good biodegradation performance of the MBR was detected when biomass reached to 7.0 μg.

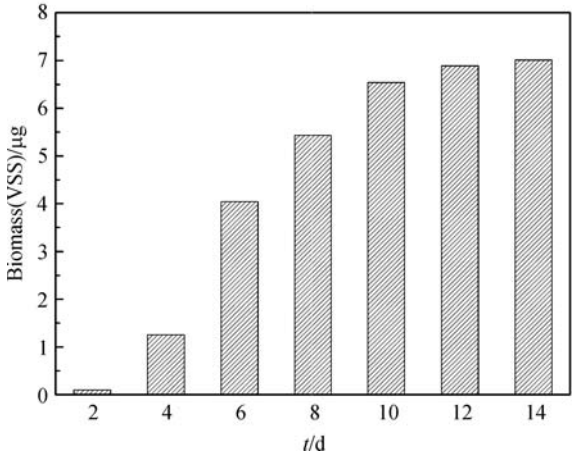

Fig. 6 The change of biomass over period of biofilm formation.

3.5 Morphology and microstructure

To further understand the start-up process, SEM was employed to visualize the biofilm morphology and microstructure of *Pseudomonas* immobilized on the membrane. SEM images of biofilm formed under different toluene concentrations are presented in Fig. 7. The predominant morphology of the bacteria in the biofilm was rods. Material resembling extracellular polymeric substance (EPS) is also visible in the image. EPS enhanced biofilm development by binding the cells together to form a complex assemblage of cells trapped within an organic matrix, together with their metabolic products. In addition, voids were clearly found to be distributed among the bacterial cells and EPS within structurally heterogeneous biofilms, these could create pathways for the transport of substrates and metabolic products and sulfur dioxide penetration.

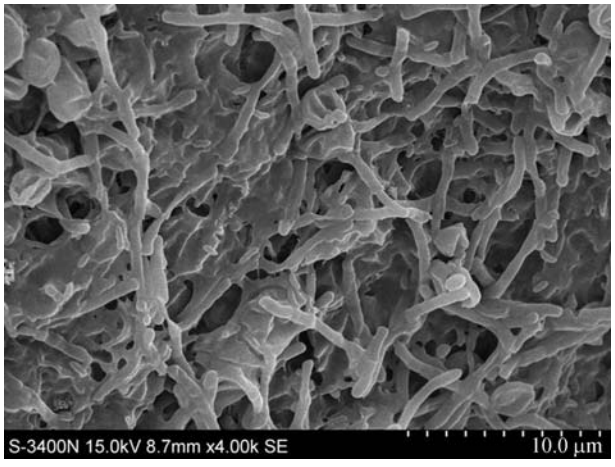

Fig. 7 SEM micrograph of the biofilm.

4 Conclusions

The start-up process of a MBR consists of three phases: a biofilm formation period (0–5 d), development period (6–10 d), and stabilization period (11–14 d). In the start-up process, the dry weight, active biomass, pressure drop and removal efficiency of the MBR initially increased, in contrast, these parameters remained relatively steady during the stabilization period. On the other hand, mature biofilm formed on the 14th day and the maximal removal efficiency was achieved and subsequently remained at 78%. Our results demonstrated that the MBR is available for flue-gas desulfurization, and also suggested that the synthetic analysis of the parameters mentioned in this work could be served as a guideline for practical biofilm formation in a MBR.

Acknowledgements This study was supported by the National Key Technology Research & Development Program (No. 2012BAK30B03) and the National Natural Science Foundation of China (Grant Nos. 41271543 and 41101564).

References

Ali A, Srivastava S K, Haque R (1992). Chemical desulphurization of high sulphur coals. Fuel, 71(7): 835–839

Bai J H, Cui B S, Chen B, Zhang K J, Deng W, Gao H F, Xiao R (2011). Spatial distribution and ecological risk assessment of heavy metals in surface sediments from a typical plateau lake wetland, China. Ecol Modell, 222(2): 301–306

Bhadra A, Scharer J M, Moo-Young M (1987). Microbial desulphurization of heavy oils and bitumen. Biotechnol Adv, 5(1): 1–27

Bos P, Huber T F, Luyben K Ch A M, Kuenen J G (1988). Feasibility of a Dutch process for microbial desulphurization of coal. Resources, Conservation and Recycling, 1(3–4): 279–291

Chen B, Chen G Q (2006a). Exergy analysis for resource conversion of the Chinese society 1993 under the material product system. Energy, 31(8–9): 1115–1150

Chen B, Chen G Q (2006b). Ecological footprint accounting based on emergy—A case study of the Chinese society. Ecological Modelling, 198(1–2): 101–114

Chen B, Chen G Q (2007). Modified ecological footprint accounting and analysis based on embodied exergy—A case study of the Chinese society 1981–2001. Ecol Econ, 61(2–3): 355–376.

Chen B, Chen G Q, Yang Z F (2006a). Exergy-based resource accounting for China. Ecological Modelling, 196(3–4): 313–328

Chen B, Chen G Q, Yang Z F, Jiang M M (2007). Ecological footprint accounting for energy and resource in China. Energy Policy, 35(3): 1599–1609

Chen B, Chen Z M, Zhou Y, Zhou J B, Chen G Q (2009). Emergy as embodied energy based assessment for local sustainability of a constructed wetland in Beijing. Commun Nonlinear Sci Numer Simul, 14(2): 622–635

Chen B, He G X, Qi J, Su M R, Zhou S Y, Jiang M M (2012a). Greenhouse gas inventory of a typical high-end industrial park in China. ScientificWorldJournal, doi: 10.1155/2013/717054

Chen B, He G X, Yang J, Zhang J R, Su M R, Qi J (2012b). Evaluating ecological and economic benefits of a low-carbon industrial park based on millennium ecosystem assessment framework. ScientificWorldJournal, doi: 10.1100/2012/909317

Chen B, Zeng L, Wu Y H, Ji P, Zhao Y J (2012c). Transport of bicomponent contaminant in free-surface wetland flow. J Hydrodynam, 24(6): 925–929

Chen G Q, Chen B (2009). Extended exergy analysis of the Chinese society. Energy, 34(9): 1127–1144

Chen G Q, Jiang M M, Chen B, Yang Z F, Lin C (2006b). Emergy analysis of Chinese agriculture. Agric Ecosyst Environ, 115(1–4): 161–173

Chen R, Liao Q, Zhu X, Wang Y Z, Liao H (2004). Visualization test for purification of toluene in biofilter with a regular porous structure. J Eng Thermophys, 25(3): 481–483

Chen S Q, Chen B (2012a). Network environ perspective for urban metabolism and carbon emissions: a case study of Vienna, Austria. Environ Sci Technol, 46(8): 4498–4506

Chen S Q, Chen B (2012b). Sustainability and future alternatives of biogas-linked agrosystem (BLAS) in China: an emergy analysis. Renew Sustain Energy Rev, 16(6): 3948–3959

Chen S Q, Chen B, Song D (2012d). Life-cycle energy production and emissions mitigation by comprehensive biogas–digestate utilization. Bioresour Technol, 114: 357–364

Chen Z M, Chen B, Chen G Q (2011). Cosmic exergy based ecological assessment for a wetland in Beijing. Ecol Modell, 222(2): 322–329

Chen Z M, Chen B, Zhou J B, Li Z, Zhou Y, Xi X R, Lin C, Chen G Q (2008). A vertical subsurface-flow constructed wetland in Beijing. Commun Nonlinear Sci Numer Simul, 13(9): 1986–1997

Chen Z M, Chen G Q, Zhou J B, Jiang M M, Chen B (2010). Ecological input-output modeling for embodied resources and emissions in Chinese economy. Commun Nonlinear Sci Numer Simul, 15(7): 1942–1965

Dai J, Fath B D, Chen B (2012). Constructing a network of the social-economic consumption system of China using extended exergy analysis. Renew Sustain Energy Rev, 16(7): 4796–4808

Eligwe C A (1988). Microbial desulphurization of coal. Fuel, 67(4): 451–458

Evrim E, Tülay D, Tijen Ö B, Yuda Y (1998). The effect of lignite type and particle size on microbial desulphurization by Rhodococcus rhodochrous. Fuel, 77(9–10): 1121–1124

Feng L, Wang D G, Chen B (2011). Water quality modeling for a tidal river network: a case study of the Suzhou River. Frontiers of Earth Science, 5(4): 428–431

He W, Zhang Y Y, Tian R, Hu H X, Chen B, Chen L K, Xu F L (2013). Modeling the purification effects of the constructed Sphagnum wetland on phosphorus and heavy metals in Dajiuhu Wetland Reserve, China. Ecol Modell, doi: 10.1016/j.ecolmodel.2012.09.025

Howell J A (2004). Future of membranes and membrane reactors in green technologies and for water reuse. Desalination, 162: 1–11

Huang L B, Bai J H, Chen B, Zhang K J, Huang C, Liu P P (2012). Two-decade wetland cultivation and its effects on soil properties in salt marshes in the Yellow River Delta, China. Ecol Inform, 10: 37–48

Huang L Q, Chen G Q, Zhang Y, Chen B, Luan S J (2007). Exergy as a unified measure of water quality. Commun Nonlinear Sci Numer Simul, 12(5): 663–672

Hubacek K, Feng K S, Chen B (2012). Changing lifestyles towards a low carbon economy: an IPAT analysis for China. Energies, 5(12): 22–31

Iranpour R, Cox H H J, Deshusses M A, Schroeder E D (2005). Literature review of air pollution control biofilters and biotrickling filters for odor and volatile organic compound removal. Environ Prog, 24(3): 254–267

Ji X, Chen G Q, Chen B, Jiang M M (2009). Exergy-based assessment for waste gas emissions from Chinese Transportation. Energy Policy, 37(6): 2231–2240

Jiang M M, Chen B, Zhou J B, Tao F R, Li Z, Yang Z F, Chen G Q (2007). Emergy account for biomass resource exploitation by agriculture in China. Energy Policy, 35(9): 4704–4719

Jiang M M, Zhou J B, Chen B, Chen G Q (2008). Emergy-based ecological account for the Chinese Economy in 2004. Commun Nonlinear Sci Numer Simul, 13(10): 2337–2356

Jiang M M, Zhou J B, Chen B, Yang Z F, Ji X, Zhang L X, Chen G Q (2009). Ecological evaluation of Beijing economy based on emergy indices. Commun Nonlinear Sci Numer Simul, 14(5): 2482–2494

Ju L P, Chen B (2011). Embodied energy and emergy evaluation of a typical biodiesel production chain in China. Ecol Modell, 222(14):

2385–2392

Kusnierova M, Prascakova M, Fecko P, Janakova I (2010). Chemical and biological desulphurization of boiler coal. J Biotechnol, 150: 252

Liu G B, Liu W J, Xu J J, Chen Z X, Tao X P (2009). Study on effects of flydust on limestone dissolution characteristics for desulfurization. Environ Sci Technol, 22(2): 26–28

Liu G B, Tan W Y, Liu W J, Tu Y, Wu W, Tao X P (2008). Dissolution of limestone in WFGD and its mathematic model. Jiangsu Environmental Science and Technology, 21(5): 26–28

Lu Y, Su M R, Liu G Y, Chen B, Zhou S Y, Jiang M M (2012). Ecological network analysis for a low-carbon and high-tech industrial park. ScientificWorldJournal, doi: 10.1100/2012/305474

Olsson G, Larsson L, Holst O, Karlsson H T (1989). Microorganisms for desulphurization of coal: the influence of leaching compounds on their growth. Fuel, 68(10): 1270–1274

Pereira M O, Morin P, Vieira M J, Melo L F (2002). A versatile reactor for continuous monitoring of biofilm properties in laboratory and industrial conditions. Lett Appl Microbiol, 34(1): 22–26

Pysh'yev S, Gunka V, Prysiazhnyi Y, Shevchuk K, Pattek-Janczyk A (2012). Study of the oxidative desulphurization process of coal with different metamorphism degrees. Journal of Fuel Chemistry and Technology, 40(2): 129–137

Qu Y H, Lin C, Zhou W, Li Y, Chen B, Chen G Q (2009a). Effects of CO_2 concentration and moisture content of sugar-free media on the tissue-cultured plantlets in large growth chamber. Commun Nonlinear Sci Numer Simul, 14(1): 322–330

Qu Y H, Wei X M, Hou Y F, Chen B, Chen G Q, Lin C (2009b). Analysis for an environmental friendly seedling breeding system. Commun Nonlinear Sci Numer Simul, 14(4): 1766–1772

Richard F, Yan J Y, Felix S, Sascha P (2011). Flue gas desulphurization for hot recycle Oxyfuel combustion: Experiences from the 30 MWth Oxyfuel pilot plant in Schwarze Pumpe. Int J Greenh Gas Control, 5: S210–S223

Song D, Su M R, Yang J, Chen B (2012). Greenhouse gas emission accounting and management of low-carbon community. ScientificWorldJournal, doi: 10.1100/2012/613721

Su M R, Chen L, Chen B, Chen S Q, Yang Z F (2012). Low-carbon development patterns: observations of typical Chinese cities. Energies, 5(2): 291–304

Sun K Q, Zhong Q (2005). The Design Construction and Operation of Gas Desulfurization System in Power Plant. Beijing: Chemical Industry Press, 105–106

Wang X, Meng L, Chen B, Yang Z F, Li C (2009a). Simulation of nitrogen contaminant transportation by a compact difference scheme in the downstream Yellow River, China. Commun Nonlinear Sci Numer Simul, 14(3): 935–945

Wang Y G, Gao D, Lin J W, Wei D Z (2005). Study on operational conditions of microorganism cultivation for flue gas desulfurization and technological properties of bioreactor start-up. Modern Chemical Industry, 25(5): 40–43

Więckowska J (1995). Catalytic and adsorptive desulphurization of gases. Catal Today, 24(4): 405–465

Xu F L, Wang J J, Chen B, Qin N, Wu W J, He W, He Q S, Wang Y (2011). The variations of exergies and structural exergies along eutrophication gradients in Chinese and Italian lakes. Ecol Modell, 222(2): 337–350

Yang J, Chen B, Qi J, Zhou S Y, Jiang M M (2012). Life-cycle-based multicriteria sustainability evaluation of industrial parks: a case study in China. ScientificWorldJournal, doi: 10.1100/2012/917830

Yang J, Chen W C, Chen B (2011b). Impacts of biogas projects on agro-ecosystem in rural areas — A case study of Gongcheng. Frontiers of Earth Science, 5(3): 317–322

Yang Q, Chen B, Ji X, He Y F, Chen G Q (2009). Exergetic evaluation of corn-ethanol production in China. Commun Nonlinear Sci Numer Simul, 14(5): 2450–2461

Yang Z F, Chen B (2011). Systematic studies on wetlands in China. Ecol Modell, 222(2): 221–223

Yang Z F, Chen B (2012). Anthropogenic impacts on multi-scale ecosystems. Ecol Inform, 10: 1, doi: 10.1016/j.ecoinf.2012.05.003

Yang Z F, Jiang M M, Chen B, Zhou J B, Chen G Q, Li S C (2010). Solar Emergy evaluation for Chinese economy. Energy Policy, 38(2): 875–886

Yu Y S, Yang J, Chen B (2012). Smart grid in China—A review. Energies, 5(12): 1321–1338

Zeng L, Wu Y H, Ji P, Chen B, Zhao Y J, Chen G Q, Wu Z (2012). Effect of wind on contaminant dispersion in a wetland flow dominated by free-surface effect. Ecol Modell, 237–238: 101–108

Zhan J, Yan H, Chen B, Luo J, Shi N (2012). Decomposing analysis of the mechanisms behind the spatial and temporal patterns of changes in carbon sequestration in China. Energies, 5(12): 386–398

Zhang D C, Zhang M X, Chen Q R (2009). Study on coal bio-magnetizing desulphurization. Procedia Earth and Planetary Science, 1(1): 673–678

Zhang L X, Feng Y Y, Chen B (2011). Alternative scenarios for the development of a low-carbon city: a case study of Beijing, China. Energies, 4(12): 2295–2310

Zhang L X, Song B, Chen B (2012). Emergy-based analysis of four farming systems: insight into agricultural diversification in rural China. J Clean Prod, 28: 33–44

Zhang X H, Zhang H W, Chen B, Chen G Q, Zhao X H (2008). Water resources strategic based on complex system dynamics: a case study of Tianjin city. Commun Nonlinear Sci Numer Simul, 13(10): 2328–2336

Zhao R, Yang Z F, Sun T, Chen B, Chen G Q (2009a). Freshwater inflow requirements for the protection of the critical habitat and the drinking water sources in the Yangtze River Estuary, China. Commun Nonlinear Sci Numer Simul, 14(5): 2507–2518

Zhao X, Chen B, Yang Z F (2009b). National water footprint in an input-output framework-a case study of China 2002. Ecol Modell, 220(2): 245–253

Zhou J B, Jiang M M, Chen B, Chen G Q (2009). Emergy evaluations for constructed wetland and conventional wastewater treatments. Commun Nonlinear Sci Numer Simul, 14(4): 1781–1789